First Measurement of the Ratio of Central-Electron to Forward-Electron *W* Partial Cross Sections in $p\bar{p}$ Collisions at $\sqrt{s} = 1.96$ TeV

A. Abulencia,[24] J. Adelman,[13] T. Affolder,[10] T. Akimoto,[55] M. G. Albrow,[17] S. Amerio,[43] D. Amidei,[35] A. Anastassov,[52] K. Anikeev,[17] A. Annovi,[19] J. Antos,[14] M. Aoki,[55] G. Apollinari,[17] T. Arisawa,[57] A. Artikov,[15] W. Ashmanskas,[17] A. Attal,[3] A. Aurisano,[42] F. Azfar,[42] P. Azzi-Bacchetta,[43] P. Azzurri,[46] N. Bacchetta,[43] W. Badgett,[17] A. Barbaro-Galtieri,[29] V. E. Barnes,[48] B. A. Barnett,[25] S. Baroiant,[7] V. Bartsch,[31] G. Bauer,[33] P.-H. Beauchemin,[34] F. Bedeschi,[46] S. Behari,[25] G. Bellettini,[46] J. Bellinger,[59] A. Belloni,[33] D. Benjamin,[16] A. Beretvas,[17] J. Beringer,[29] T. Berry,[30] A. Bhatti,[50] M. Binkley,[17] D. Bisello,[43] I. Bizjak,[31] R. E. Blair,[2] C. Blocker,[6] B. Blumenfeld,[25] A. Bocci,[16] A. Bodek,[49] V. Boisvert,[49] G. Bolla,[48] A. Bolshov,[33] D. Bortoletto,[48] J. Boudreau,[47] A. Boveia,[10] B. Brau,[10] L. Brigliadori,[5] C. Bromberg,[36] E. Brubaker,[13] J. Budagov,[15] H. S. Budd,[49] S. Budd,[24] K. Burkett,[17] G. Busetto,[43] P. Bussey,[21] A. Buzatu,[34] K. L. Byrum,[2] S. Cabrera,[16,q] M. Campanelli,[20] M. Campbell,[35] F. Canelli,[17] A. Canepa,[45] S. Carillo,[18,i] D. Carlsmith,[59] R. Carosi,[46] S. Carron,[34] B. Casal,[11] M. Casarsa,[54] A. Castro,[5] P. Catastini,[46] D. Cauz,[54] M. Cavalli-Sforza,[3] A. Cerri,[29] L. Cerrito,[31,m] S. H. Chang,[28] Y. C. Chen,[1] M. Chertok,[7] G. Chiarelli,[46] G. Chlachidze,[17] F. Chlebana,[17] I. Cho,[28] K. Cho,[28] D. Chokheli,[15] J. P. Chou,[22] G. Choudalakis,[33] S. H. Chuang,[52] K. Chung,[12] W. H. Chung,[59] Y. S. Chung,[49] M. Cilijak,[46] C. I. Ciobanu,[24] M. A. Ciocci,[46] A. Clark,[20] D. Clark,[6] M. Coca,[16] G. Compostella,[43] M. E. Convery,[50] J. Conway,[7] B. Cooper,[31] K. Copic,[35] M. Cordelli,[19] G. Cortiana,[43] F. Crescioli,[46] C. Cuenca Almenar,[7,q] J. Cuevas,[11,l] R. Culbertson,[17] J. C. Cully,[35] S. DaRonco,[43] M. Datta,[17] S. D'Auria,[21] T. Davies,[21] D. Dagenhart,[17] P. de Barbaro,[49] S. De Cecco,[51] A. Deisher,[29] G. De Lentdecker,[49,c] G. De Lorenzo,[3] M. Dell'Orso,[46] F. Delli Paoli,[43] L. Demortier,[50] J. Deng,[16] M. Deninno,[5] D. De Pedis,[51] P. F. Derwent,[17] G. P. Di Giovanni,[44] C. Dionisi,[51] B. Di Ruzza,[54] J. R. Dittmann,[4] M. D'Onofrio,[3] C. Dörr,[26] S. Donati,[46] P. Dong,[8] J. Donini,[43] T. Dorigo,[43] S. Dube,[52] J. Efron,[39] R. Erbacher,[7] D. Errede,[24] S. Errede,[24] R. Eusebi,[17] H. C. Fang,[29] S. Farrington,[30] I. Fedorko,[46] W. T. Fedorko,[13] R. G. Feild,[60] M. Feindt,[26] J. P. Fernandez,[32] R. Field,[18] G. Flanagan,[48] R. Forrest,[7] S. Forrester,[7] M. Franklin,[22] J. C. Freeman,[29] I. Furic,[13] M. Gallinaro,[50] J. Galyardt,[12] J. E. Garcia,[46] F. Garberson,[10] A. F. Garfinkel,[48] C. Gay,[60] H. Gerberich,[24] D. Gerdes,[35] S. Giagu,[51] P. Giannetti,[46] K. Gibson,[47] J. L. Gimmell,[49] C. Ginsburg,[17] N. Giokaris,[15,a] M. Giordani,[54] P. Giromini,[19] M. Giunta,[46] G. Giurgiu,[25] V. Glagolev,[15] D. Glenzinski,[17] M. Gold,[37] N. Goldschmidt,[18] J. Goldstein,[42,b] A. Golossanov,[17] G. Gomez,[11] G. Gomez-Ceballos,[33] M. Goncharov,[53] O. González,[32] I. Gorelov,[37] A. T. Goshaw,[16] K. Goulianos,[50] A. Gresele,[43] S. Grinstein,[22] C. Grosso-Pilcher,[13] R. C. Group,[17] U. Grundler,[24] J. Guimaraes da Costa,[22] Z. Gunay-Unalan,[36] C. Haber,[29] K. Hahn,[33] S. R. Hahn,[17] E. Halkiadakis,[52] A. Hamilton,[20] B.-Y. Han,[49] J. Y. Han,[49] R. Handler,[59] F. Happacher,[19] K. Hara,[55] D. Hare,[52] M. Hare,[56] S. Harper,[42] R. F. Harr,[58] R. M. Harris,[17] M. Hartz,[47] K. Hatakeyama,[50] J. Hauser,[8] C. Hays,[42] M. Heck,[26] A. Heijboer,[45] B. Heinemann,[29] J. Heinrich,[45] C. Henderson,[33] M. Herndon,[59] J. Heuser,[26] D. Hidas,[16] C. S. Hill,[10,b] D. Hirschbuehl,[26] A. Hocker,[17] A. Holloway,[22] S. Hou,[1] M. Houlden,[30] S.-C. Hsu,[9] B. T. Huffman,[42] R. E. Hughes,[39] U. Husemann,[60] J. Huston,[36] J. Incandela,[10] G. Introzzi,[46] M. Iori,[51] A. Ivanov,[7] B. Iyutin,[33] E. James,[17] D. Jang,[52] B. Jayatilaka,[16] D. Jeans,[51] E. J. Jeon,[28] S. Jindariani,[18] W. Johnson,[7] M. Jones,[48] K. K. Joo,[28] S. Y. Jun,[12] J. E. Jung,[28] T. R. Junk,[24] T. Kamon,[53] P. E. Karchin,[58] Y. Kato,[41] Y. Kemp,[26] R. Kephart,[17] U. Kerzel,[26] V. Khotilovich,[53] B. Kilminster,[39] D. H. Kim,[28] H. S. Kim,[28] J. E. Kim,[28] M. J. Kim,[17] S. B. Kim,[28] S. H. Kim,[55] Y. K. Kim,[13] N. Kimura,[55] L. Kirsch,[6] S. Klimenko,[18] M. Klute,[33] B. Knuteson,[33] B. R. Ko,[16] K. Kondo,[57] D. J. Kong,[28] J. Konigsberg,[18] A. Korytov,[18] A. V. Kotwal,[16] A. C. Kraan,[45] J. Kraus,[24] M. Kreps,[26] J. Kroll,[45] N. Krumnack,[4] M. Kruse,[16] V. Krutelyov,[10] T. Kubo,[55] S. E. Kuhlmann,[2] T. Kuhr,[26] N. P. Kulkarni,[58] Y. Kusakabe,[57] S. Kwang,[13] A. T. Laasanen,[48] S. Lai,[34] S. Lami,[46] S. Lammel,[17] M. Lancaster,[31] R. L. Lander,[7] K. Lannon,[39] A. Lath,[52] G. Latino,[46] I. Lazzizzera,[43] T. LeCompte,[2] J. Lee,[49] J. Lee,[28] Y. J. Lee,[28] S. W. Lee,[53,o] R. Lefèvre,[20] N. Leonardo,[33] S. Leone,[46] S. Levy,[13] J. D. Lewis,[17] C. Lin,[60] C. S. Lin,[17] M. Lindgren,[17] E. Lipeles,[9] A. Lister,[7] D. O. Litvintsev,[17] T. Liu,[17] N. S. Lockyer,[45] A. Loginov,[60] M. Loreti,[43] R.-S. Lu,[1] D. Lucchesi,[43] P. Lujan,[29] P. Lukens,[17] G. Lungu,[18] L. Lyons,[42] J. Lys,[29] R. Lysak,[14] E. Lytken,[48] P. Mack,[26] D. MacQueen,[34] R. Madrak,[17] K. Maeshima,[17] K. Makhoul,[33] T. Maki,[23] P. Maksimovic,[25] S. Malde,[42] S. Malik,[31] G. Manca,[30] A. Manousakis,[15,a] F. Margaroli,[5] R. Marginean,[17] C. Marino,[26] C. P. Marino,[24] A. Martin,[60] M. Martin,[25] V. Martin,[21,g] M. Martínez,[3] R. Martínez-Ballarín,[32] T. Maruyama,[55] P. Mastrandrea,[51] T. Masubuchi,[55] H. Matsunaga,[55] M. E. Mattson,[58] R. Mazini,[34] P. Mazzanti,[5] K. S. McFarland,[49] P. McIntyre,[53] R. McNulty,[30,f] A. Mehta,[30] P. Mehtala,[23] S. Menzemer,[11,h] A. Menzione,[46] P. Merkel,[48] C. Mesropian,[50] A. Messina,[36] T. Miao,[17] N. Miladinovic,[6] J. Miles,[33] R. Miller,[36] C. Mills,[10] M. Milnik,[26] A. Mitra,[1] G. Mitselmakher,[18] A. Miyamoto,[27] S. Moed,[20] N. Moggi,[5] B. Mohr,[8] C. S. Moon,[28] R. Moore,[17] M. Morello,[46]

P H Y S I C A L   R E V I E W   L E T T E R S

P. Movilla Fernandez,[29] J. Mülmenstädt,[29] A. Mukherjee,[17] Th. Muller,[26] R. Mumford,[25] P. Murat,[17] M. Mussini,[5]
J. Nachtman,[17] A. Nagano,[55] J. Naganoma,[57] K. Nakamura,[55] I. Nakano,[40] A. Napier,[56] V. Necula,[16] C. Neu,[45]
M. S. Neubauer,[9] J. Nielsen,[29,n] L. Nodulman,[2] O. Norniella,[3] E. Nurse,[31] S. H. Oh,[16] Y. D. Oh,[28] I. Oksuzian,[18]
T. Okusawa,[41] R. Oldeman,[30] R. Orava,[23] K. Osterberg,[23] C. Pagliarone,[46] E. Palencia,[11] V. Papadimitriou,[17]
A. Papaikonomou,[26] A. A. Paramonov,[13] B. Parks,[39] S. Pashapour,[34] J. Patrick,[17] G. Pauletta,[54] M. Paulini,[12] C. Paus,[33]
D. E. Pellett,[7] A. Penzo,[54] T. J. Phillips,[16] G. Piacentino,[46] J. Piedra,[44] L. Pinera,[18] K. Pitts,[24] C. Plager,[8] L. Pondrom,[59]
X. Portell,[3] O. Poukhov,[15] N. Pounder,[42] F. Prakoshyn,[15] A. Pronko,[17] J. Proudfoot,[2] F. Ptohos,[19,e] G. Punzi,[46] J. Pursley,[25]
J. Rademacker,[42,b] A. Rahaman,[47] V. Ramakrishnan,[59] N. Ranjan,[48] I. Redondo,[32] B. Reisert,[17] V. Rekovic,[37] P. Renton,[42]
M. Rescigno,[51] S. Richter,[26] F. Rimondi,[5] L. Ristori,[46] A. Robson,[21] T. Rodrigo,[11] E. Rogers,[24] S. Rolli,[56] R. Roser,[17]
M. Rossi,[54] R. Rossin,[10] P. Roy,[34] A. Ruiz,[11] J. Russ,[12] V. Rusu,[13] H. Saarikko,[23] A. Safonov,[53] W. K. Sakumoto,[49]
G. Salamanna,[51] O. Saltó,[3] L. Santi,[54] S. Sarkar,[51] L. Sartori,[46] K. Sato,[17] P. Savard,[34] A. Savoy-Navarro,[44] T. Scheidle,[26]
P. Schlabach,[17] E. E. Schmidt,[17] M. P. Schmidt,[60] M. Schmitt,[38] T. Schwarz,[7] L. Scodellaro,[11] A. L. Scott,[10] A. Scribano,[46]
F. Scuri,[46] A. Sedov,[48] S. Seidel,[37] Y. Seiya,[41] A. Semenov,[15] L. Sexton-Kennedy,[17] A. Sfyrla,[20] S. Z. Shalhout,[58]
M. D. Shapiro,[29] T. Shears,[30] P. F. Shepard,[47] D. Sherman,[22] M. Shimojima,[55,k] M. Shochet,[13] Y. Shon,[59] I. Shreyber,[20]
A. Sidoti,[46] P. Sinervo,[34] A. Sisakyan,[15] A. J. Slaughter,[17] J. Slaunwhite,[39] K. Sliwa,[56] J. R. Smith,[7] F. D. Snider,[17]
R. Snihur,[34] M. Soderberg,[35] A. Soha,[7] S. Somalwar,[52] V. Sorin,[36] J. Spalding,[17] F. Spinella,[46] T. Spreitzer,[34]
P. Squillacioti,[46] M. Stanitzki,[60] A. Staveris-Polykalas,[46] R. St. Denis,[21] B. Stelzer,[8] O. Stelzer-Chilton,[42] D. Stentz,[38]
J. Strologas,[37] D. Stuart,[10] J. S. Suh,[28] A. Sukhanov,[18] H. Sun,[56] I. Suslov,[15] T. Suzuki,[55] A. Taffard,[24,p] R. Takashima,[40]
Y. Takeuchi,[55] R. Tanaka,[40] M. Tecchio,[35] P. K. Teng,[1] K. Terashi,[50] J. Thom,[17,d] A. S. Thompson,[21] E. Thomson,[45]
P. Tipton,[60] V. Tiwari,[12] S. Tkaczyk,[17] D. Toback,[53] S. Tokar,[14] K. Tollefson,[36] T. Tomura,[55] D. Tonelli,[46] S. Torre,[19]
D. Torretta,[17] S. Tourneur,[44] W. Trischuk,[34] S. Tsuno,[40] Y. Tu,[45] N. Turini,[46] F. Ukegawa,[55] S. Uozumi,[55] S. Vallecorsa,[20]
N. van Remortel,[23] A. Varganov,[35] E. Vataga,[37] F. Vazquez,[18,i] G. Velev,[17] C. Vellidis,[46,a] G. Veramendi,[24] V. Veszpremi,[48]
M. Vidal,[32] R. Vidal,[17] I. Vila,[11] R. Vilar,[11] T. Vine,[31] I. Vollrath,[34] I. Volobouev,[29,o] G. Volpi,[46] F. Würthwein,[9]
P. Wagner,[53] R. G. Wagner,[2] R. L. Wagner,[17] J. Wagner,[26] W. Wagner,[26] R. Wallny,[8] S. M. Wang,[1] A. Warburton,[34]
D. Waters,[31] M. Weinberger,[53] W. C. Wester III,[17] B. Whitehouse,[56] D. Whiteson,[45] A. B. Wicklund,[2] E. Wicklund,[17]
G. Williams,[34] H. H. Williams,[45] P. Wilson,[17] B. L. Winer,[39] P. Wittich,[17,d] S. Wolbers,[17] C. Wolfe,[13] T. Wright,[35] X. Wu,[20]
S. M. Wynne,[30] A. Yagil,[9] K. Yamamoto,[41] J. Yamaoka,[52] T. Yamashita,[40] C. Yang,[60] U. K. Yang,[13,j] Y. C. Yang,[28]
W. M. Yao,[29] G. P. Yeh,[17] J. Yoh,[17] K. Yorita,[13] T. Yoshida,[41] G. B. Yu,[49] I. Yu,[28] S. S. Yu,[17] J. C. Yun,[17] L. Zanello,[51]
A. Zanetti,[54] I. Zaw,[22] X. Zhang,[24] J. Zhou,[52] and S. Zucchelli[5]

(CDF Collaboration)

[1]*Institute of Physics, Academia Sinica, Taipei, Taiwan 11529, Republic of China*
[2]*Argonne National Laboratory, Argonne, Illinois 60439, USA*
[3]*Institut de Fisica d'Altes Energies, Universitat Autonoma de Barcelona, E-08193, Bellaterra (Barcelona), Spain*
[4]*Baylor University, Waco, Texas 76798, USA*
[5]*Istituto Nazionale di Fisica Nucleare, University of Bologna, I-40127 Bologna, Italy*
[6]*Brandeis University, Waltham, Massachusetts 02254, USA*
[7]*University of California, Davis, Davis, California 95616, USA*
[8]*University of California, Los Angeles, Los Angeles, California 90024, USA*
[9]*University of California, San Diego, La Jolla, California 92093, USA*
[10]*University of California, Santa Barbara, Santa Barbara, California 93106, USA*
[11]*Instituto de Fisica de Cantabria, CSIC-University of Cantabria, 39005 Santander, Spain*
[12]*Carnegie Mellon University, Pittsburgh, Pennsylvania 15213, USA*
[13]*Enrico Fermi Institute, University of Chicago, Chicago, Illinois 60637, USA*
[14]*Comenius University, 842 48 Bratislava, Slovakia; Institute of Experimental Physics, 040 01 Kosice, Slovakia*
[15]*Joint Institute for Nuclear Research, RU-141980 Dubna, Russia*
[16]*Duke University, Durham, North Carolina 27708, USA*
[17]*Fermi National Accelerator Laboratory, Batavia, Illinois 60510, USA*
[18]*University of Florida, Gainesville, Florida 32611, USA*
[19]*Laboratori Nazionali di Frascati, Istituto Nazionale di Fisica Nucleare, I-00044 Frascati, Italy*
[20]*University of Geneva, CH-1211 Geneva 4, Switzerland*
[21]*Glasgow University, Glasgow G12 8QQ, United Kingdom*
[22]*Harvard University, Cambridge, Massachusetts 02138, USA*

[23]*Division of High Energy Physics, Department of Physics, University of Helsinki and Helsinki Institute of Physics, FIN-00014, Helsinki, Finland*

[24]*University of Illinois, Urbana, Illinois 61801, USA*

[25]*The Johns Hopkins University, Baltimore, Maryland 21218, USA*

[26]*Institut für Experimentelle Kernphysik, Universität Karlsruhe, 76128 Karlsruhe, Germany*

[27]*High Energy Accelerator Research Organization (KEK), Tsukuba, Ibaraki 305, Japan*

[28]*Center for High Energy Physics: Kyungpook National University, Taegu 702-701, Korea;
Seoul National University, Seoul 151-742, Korea;
SungKyunKwan University, Suwon 440-746, Korea*

[29]*Ernest Orlando Lawrence Berkeley National Laboratory, Berkeley, California 94720, USA*

[30]*University of Liverpool, Liverpool L69 7ZE, United Kingdom*

[31]*University College London, London WC1E 6BT, United Kingdom*

[32]*Centro de Investigaciones Energeticas Medioambientales y Tecnologicas, E-28040 Madrid, Spain*

[33]*Massachusetts Institute of Technology, Cambridge, Massachusetts 02139, USA*

[34]*Institute of Particle Physics: McGill University, Montréal, Canada H3A 2T8;
University of Toronto, Toronto, Canada M5S 1A7*

[35]*University of Michigan, Ann Arbor, Michigan 48109, USA*

[36]*Michigan State University, East Lansing, Michigan 48824, USA*

[37]*University of New Mexico, Albuquerque, New Mexico 87131, USA*

[38]*Northwestern University, Evanston, Illinois 60208, USA*

[39]*The Ohio State University, Columbus, Ohio 43210, USA*

[40]*Okayama University, Okayama 700-8530, Japan*

[41]*Osaka City University, Osaka 588, Japan*

[42]*University of Oxford, Oxford OX1 3RH, United Kingdom*

[43]*Istituto Nazionale di Fisica Nucleare, Sezione di Padova-Trento, University of Padova, I-35131 Padova, Italy*

[44]*LPNHE, Universite Pierre et Marie Curie/IN2P3-CNRS, UMR7585, Paris, F-75252 France*

[45]*University of Pennsylvania, Philadelphia, Pennsylvania 19104, USA*

[46]*Istituto Nazionale di Fisica Nucleare Pisa, Universities of Pisa, Siena and Scuola Normale Superiore, I-56127 Pisa, Italy*

[47]*University of Pittsburgh, Pittsburgh, Pennsylvania 15260, USA*

[48]*Purdue University, West Lafayette, Indiana 47907, USA*

[49]*University of Rochester, Rochester, New York 14627, USA*

[50]*The Rockefeller University, New York, New York 10021, USA*

[51]*Istituto Nazionale di Fisica Nucleare, Sezione di Roma 1, University of Rome "La Sapienza," I-00185 Roma, Italy*

[52]*Rutgers University, Piscataway, New Jersey 08855, USA*

[53]*Texas A&M University, College Station, Texas 77843, USA*

[54]*Istituto Nazionale di Fisica Nucleare, University of Trieste/Udine, Italy*

[55]*University of Tsukuba, Tsukuba, Ibaraki 305, Japan*

[56]*Tufts University, Medford, Massachusetts 02155, USA*

[57]*Waseda University, Tokyo 169, Japan*

[58]*Wayne State University, Detroit, Michigan 48201, USA*

[59]*University of Wisconsin, Madison, Wisconsin 53706, USA*

[60]*Yale University, New Haven, Connecticut 06520, USA*

We present a measurement of $\sigma(p\bar{p} \to W) \times \mathcal{B}(W \to e\nu)$ at $\sqrt{s} = 1.96$ TeV, using electrons identified in the forward region ($1.2 < |\eta| < 2.8$) of the CDF II detector, in 223 pb^{-1} of data. We measure $\sigma \times \mathcal{B} = 2796 \pm 13(\text{stat})^{+95}_{-90}(\text{syst}) \pm 162(\text{lum})$ pb. Combining this result with a previous CDF measurement obtained using electrons in the central region ($|\eta| \lesssim 1$), we present the first measurement of the ratio of central-electron to forward-electron W partial cross sections $R_{\text{exp}} = 0.925 \pm 0.006(\text{stat}) \pm 0.032(\text{syst})$, consistent with theoretical predictions using Coordinated Theoretical-Experimental Project on QCD (CTEQ) and Martin-Roberts-Stirling-Thorne (MRST) parton distribution functions.

The cross section for W boson production in $p\bar{p}$ collisions has been computed at next-to-leading order (NLO) [1] and next-to-next-to-leading order (NNLO) [2] in the strong coupling constant α_s. Experimental results can be used to test the calculation of higher-order QCD contributions and the parton distribution functions (PDFs) of the proton. The PDFs describe the momentum distributions of the elementary constituents of the colliding hadrons and are obtained from various parametrized fits to many sets of experimental data. Their uncertainties affect precision measurements like the masses and production cross sections of the W boson and the top quark, at both the Tevatron
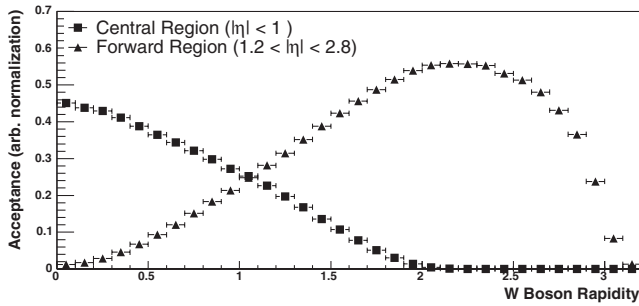
FIG. 1.   Acceptance, obtained from simulation, as a function of the W boson rapidity, $A(y_W)$. "Forward Region" refers to this measurement (electron pseudorapidity $1.2 < |\eta| < 2.8$) while "Central Region" refers to the analysis reported in [7] ($|\eta| < 1$). The two analyses sample different regions of y_W.

and the LHC [3]. Moreover, accurate PDF modeling of the pseudorapidity η [4] of the lepton from W decay is required for the use of W production as a luminosity monitor, an attractive option at the LHC [5].

The momentum fractions carried by the partons in colliding hadrons determine the momentum distribution of the W boson. The W boson momentum parallel to the proton beam direction cannot be measured in $p\bar{p}$ collisions, since the longitudinal momentum of the neutrino from the W decay is not measured. A previous measurement of the forward-backward charge asymmetry of leptons from Ws has been used to obtain some input on the momentum fraction dependence of the u and d quark PDFs within the proton [6]. Independent measurements of the W cross section with central and forward leptons provide additional sensitivity to the W rapidity y_W (Fig. 1) and are a novel way to constrain the PDFs. We present the first attempt to constrain PDFs using the ratio of W boson cross sections measured with central and forward electrons. The largest experimental uncertainty, due to luminosity, cancels in this ratio. We compare our measurement to the theoretical predictions obtained with two of the most commonly used PDF sets.

The W cross section measurement presented in this Letter is obtained using 223 ± 13 pb^{-1} of data collected by the CDF II detector during run II of the Tevatron at $\sqrt{s} = 1.96$ TeV. W bosons are identified by their decays to electrons in the forward region ($1.2 < |\eta| < 2.8$), from which we obtain the inclusive cross section times branching fraction $\sigma(p\bar{p} \to W) \times \mathcal{B}(W \to e\nu)$.

Previous run II results on W production, based on electrons with $|\eta| \lesssim 1$, were reported by both the CDF and D0 Collaborations [7,8]. In run I, at $\sqrt{s} = 1.8$ TeV, D0 reported a measurement based on electrons at $|\eta| < 1.1$ and $1.5 < |\eta| < 2.5$ [9], without separating the central from the forward regions.

The CDF II detector is described in detail elsewhere [10]. Tracking detectors inside a 1.4 T solenoidal magnetic field reconstruct the charged particles' trajectories (tracks) and measure their momenta. The silicon tracking system

(SVX) [11] provides precise measurement points from up to 8 radial layers of strip sensors. Outside the SVX is the central drift chamber (COT), which provides track measurements (hits) in 96 radial layers [12]. The COT allows full track reconstruction in the range $|\eta| < 1$. The SVX extends the track reconstruction capability up to $|\eta| \simeq 2.8$. Outside the tracking system, electromagnetic (EM) and hadronic (HAD) calorimeters measure the energy of showering particles [13]. In the forward region, the position of the EM shower is measured by two layers of scintillating strips (PES) [14]. The first layer of the forward EM calorimeter is used as a preshower detector [13]. Gas Cherenkov counters are used to determine the luminosity, with an uncertainty of 5.8% [15,16]. The trigger system has three levels [17,18]. Data used in this analysis are selected by a trigger requiring missing transverse energy $\not{E}_T > 15$ GeV and an EM cluster in the forward calorimeter with $E_T > 20$ GeV.

The offline selection of candidate W decays begins by requiring an energy cluster with $E_T > 20$ GeV in the fiducial region of the forward calorimeter at $1.2 < |\eta| < 2.8$. The ratio of hadronic to electromagnetic energy deposition must be small: $E_{\text{HAD}}/E_{\text{EM}} < 0.05$. The EM cluster is required to be isolated [19]. The neutrino from the W decay is identified by requiring $\not{E}_T > 25$ GeV.

To reduce the large remaining background, we compare the location and the energy deposition of the EM clusters in the calorimeter to projections of three-dimensional tracks independently reconstructed by the tracking detectors. Our track sample is dominated by tracks seeded by the SVX [20]. Typically, tracks in the region $1.2 < |\eta| < 1.6$ have COT hit information, while those at larger $|\eta|$ do not. The candidate events are required to have at least one track that extrapolates to the EM cluster shower centroid in the PES detector within 3 cm in the x and y coordinates. The selection is optimized by using a $Z \to ee$ data sample where one electron is detected in the central calorimeter [19] and the other one in the forward calorimeter ($Z \to ee$ control sample). The probability for matching a track to an EM cluster detected in the forward region in $Z \to ee$ events is $49.2 \pm 0.5\%$. The z coordinate of the track intersection with the beam axis must be within 60 cm from the detector center. Finally, electron candidates must satisfy $E/p < 2$. After all requirements the sample contains 48 165 events.

The kinematic and geometric acceptance (A) for $W \to e\nu$ events is determined using the PYTHIA event generator [21] and a full simulation of the CDF II detector based on the GEANT simulation package [22]. We extract $A(y_W)$ from the simulation and convolve it with a NNLO calculation of $d\sigma/dy_W$ [23]. We compute the central value of the acceptance using the MRST 2001 next-to-next-to-leading-log (NNLL) PDF set [24] (in analogy with the W cross section measurement in the central region [19]) and find $A = 0.2567 \pm 0.0002$. Two different sets of next-to-leading-log (NLL) PDFs are available (MRST01E and CTEQ6.1

[25]). To encode uncertainties in the PDF data and disagreements between measurements included in the fits, the PDF sets provide eigenvectors formed in the space of the fit parameters (20 eigenvectors for CTEQ and 15 for MRST). For each eigenvector, two complete PDF sets are provided corresponding to the changes in each direction of that eigenvector. To estimate the uncertainty due to the choice of the PDFs we convolve $A(y_W)$ with the NLO $d\sigma/dy_W$ [19] for each PDF central value and $\pm 1\sigma$ eigenvalue. Using the CTEQ6.1 eigenvector basis set, we obtain a contribution to the acceptance uncertainty of $(+1.7, -1.3)\%$. This value is roughly twice that obtained using the MRST01E PDF set. We use the difference between the NNLO and NLO $d\sigma/dy_W$ calculations to estimate the acceptance uncertainty due to higher-order QCD corrections ($\pm 0.47\%$). The other uncertainties on A are described below.

The vector sum of the energy of hadrons recoiling against the W boson enters the calculation of $\not{E}_T$. We tune the detector response to these hadrons by applying scale factors and offsets to the components of their summed energy parallel and perpendicular to the lepton momentum vector. We obtain a systematic uncertainty of $\pm 0.35\%$ on A by taking a variation corresponding to 3 standard deviations in the tuning parameters.

The energy scale and resolution modeling of electrons are calibrated with $Z \to ee$ events and result in an uncertainty of $\pm 0.24\%$. The uncertainty on the scale as a function of E_T is determined using the E/p distribution. The simulation models the E_T dependence well, and we include a $\pm 0.26\%$ uncertainty on A due to the statistical limitations of the constraint.

We vary the amount of material that an electron passes through by $\pm 1/3$ of a radiation length, based on measurements of electron energy deposition in the preshower detector. The resulting contribution to the acceptance uncertainty is $\pm 0.71\%$.

Differences in primary vertex reconstruction efficiency between data and simulation contribute less than 0.1% to the acceptance uncertainty. Finally, we vary the parameters of the PYTHIA model which influence the W boson p_T distribution [19] within the constraints of a CDF run I Z boson measurement and find the corresponding acceptance uncertainty to be less than 0.1%.

Electron identification, track matching, and E/p efficiencies are measured using the $Z \to ee$ control sample. The track matching efficiency is corrected to account for the small kinematic differences of the Z electrons with respect to those from W decay and the η distribution of electrons coming from Ws. These efficiencies contribute the largest experimental uncertainty to the cross section measurement and are limited by the Z statistics and the understanding of the background in the $Z \to ee$ sample. The relative uncertainties on the cross section measurement from electron identification, track matching, and E/p

TABLE I. Geometric and kinematic acceptance, overall efficiency, and expected number of background events.

Background multijet	$846 \pm 57(\text{stat}) \pm 423(\text{syst})$
Background $Z \to ee$	$417 \pm 5(\text{stat})$
Background $W \to \tau\nu$	$1070 \pm 12(\text{stat})$
Acceptance A	$0.2567 \pm 0.0002(\text{stat})^{+0.0051}_{-0.0042}(\text{syst})$
Efficiency ϵ_{TOT}	$0.2863 \pm 0.0042(\text{stat})^{+0.0060}_{-0.0061}(\text{syst})$

are 2.0%, 1.1%, and 1.0%, respectively. The trigger efficiency is also measured from data, using independent triggers, and results in a relative uncertainty of 0.4%. The overall efficiency is reported in Table I.

Backgrounds fall into two categories: multijet events, where one jet mimics an isolated high-p_T electron and another jet is mismeasured in the calorimeters causing $\not{E}_T$, and electroweak backgrounds, $Z \to ee$ and $W \to \tau\nu$.

The multijet background is estimated from data. Multijet events are characterized by significant energy in the cone around the electron and small $\not{E}_T$ [19]. We assume that these two variables are not correlated and estimate the number of background events in the signal region using control regions defined by either low $\not{E}_T$ or high energy in the isolation cone. We vary the cuts on $\not{E}_T$ and isolation that define the control region and obtain a relative systematic uncertainty of 50% on the multijet background estimate of 1.8%. We check this calculation by determining the fraction of jets that pass our electron criteria and applying this fraction to multijet events with large $\not{E}_T$. We obtain good agreement.

The electroweak backgrounds are estimated using simulation. We separately calculate the fraction of $Z \to ee$ and $W \to \tau\nu$ events passing our selection. These fractions are then normalized to data using the theoretical value for the ratio of $\sigma(Z)/\sigma(W)$ [2] and assuming lepton universality for the $W \to \tau\nu$ decays. Background fractions from these processes are estimated to be 2.2% and 0.9% for $W \to \tau\nu$ and $Z \to ee$, respectively.

We show the M_T [4] distribution for both the signal and background contributions in Fig. 2. The sum of signal simulation and background matches the data well.

From the number of selected events, the luminosity of the sample, the acceptance, efficiencies, and backgrounds [19] (see Table I), we measure the inclusive cross section to be $\sigma \times \mathcal{B} = 2796 \pm 13(\text{stat})^{+95}_{-90}(\text{syst}) \pm 162(\text{lum})$ pb, consistent with previous CDF results and with theoretical predictions [19]. The correct PDF must give the same total W cross section for central and forward electrons, within statistical and systematic uncertainties. It follows that the ratio of partial cross sections $\sigma_p = \sigma \times \mathcal{B} \times A$, where A is the kinematic and geometric acceptance, is equal to the true ratio of acceptances for the two regions. This experimental ratio can then be compared with acceptance ratios predicted by any set of PDFs. The cross section based on
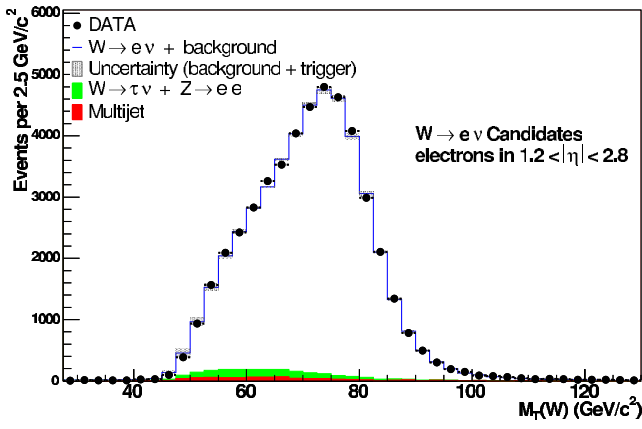
FIG. 2 (color online). M_T distribution for $W \rightarrow e\nu$ candidates (●). The histogram is the sum of the expected background and the predicted (from simulation) signal spectrum.
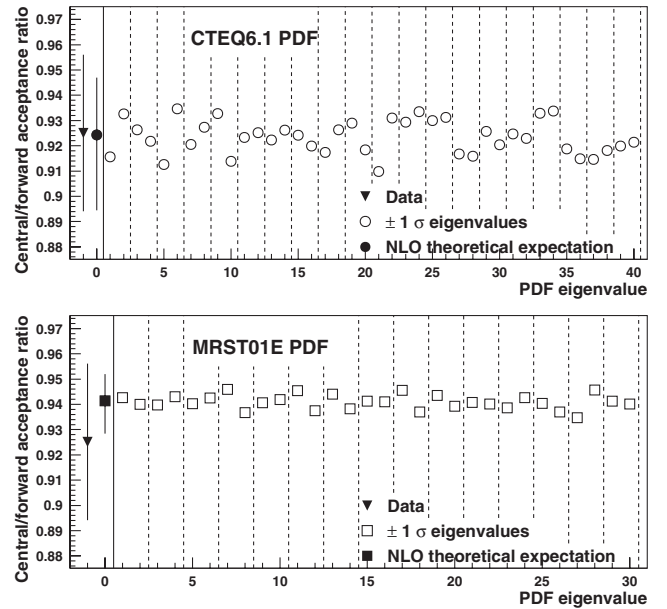

FIG. 3. The ratio of central-to-forward acceptances, as a function of the $\pm 1\sigma$ eigenvalue of CTEQ6.1 (top) and MRST01E (bottom) PDF sets. Dashed lines separate eigenvectors.

central electrons, using the same PDF as used above for the forward-electron measurement [19], is $\sigma \times \mathcal{B} = 2771 \pm 14(\text{stat}) \pm 47(\text{syst})$ pb, after removing uncertainties due to PDFs, luminosity, renormalization scale, and NLO/NNLO effects. The resulting σ_p, measured for reconstructed electrons with $E_T > 25$ GeV, $|\eta| \lesssim 1$ [7], and $\not{E}_T > 25$ GeV is $\sigma_p^{\text{cen}} = 664 \pm 3(\text{stat}) \pm 11(\text{syst})$ pb. In the forward region σ_p for $E_T > 20$ GeV, $1.2 < |\eta| < 2.8$, and $\not{E}_T > 25$ GeV is $\sigma_p^{\text{for}} = 718 \pm 3(\text{stat}) \pm 21(\text{syst})$ pb. All systematic uncertainties except those due to PDF and to NLO/NNLO effects are assigned to σ_p. Most of the luminosity uncertainty for the overlapping data-taking period cancels in the ratio, and we assign a 1% systematic due to time-dependent luminosity uncertainty. All other uncertainties are uncorrelated. The experimental ratio is $R_{\text{exp}} = \sigma_p^{\text{cen}}/\sigma_p^{\text{for}} = 0.925 \pm 0.006(\text{stat}) \pm 0.032(\text{syst})$. We compute also the central-to-forward ratio of acceptances R_{th}, obtained with two different PDF sets (CTEQ6.1 and MRST01E) at NLO level. For CTEQ6.1 the ratio is $R_{\text{th}} = 0.924^{+0.023}_{-0.030}(\text{PDF}) \pm 0.004$ (NLO/NNLO) and for MRST01E $R_{\text{th}} = 0.941^{+0.010}_{-0.012}(\text{PDF}) \pm 0.004$ (NLO/NNLO), where "PDF" indicates the uncertainty obtained by varying the eigenvalues relative to a given PDF set.

Figure 3 shows the experimental ratio of partial cross sections (solid triangles) compared to the CTEQ6.1 (upper plot) and MRST01E (lower plot) acceptance ratios (solid circle and square). The data measurement is independent of PDFs. The ratios of acceptances are also computed varying each PDF eigenvalue by $\pm 1\sigma$ (giving 40 values for CTEQ6.1 and 30 for MRST01E, shown as open circles and squares). Data and both PDF sets agree within uncertainties, though the central values for MRST01E and CTEQ6.1 are slightly shifted with respect to each other. The CTEQ6.1 has a larger uncertainty and some of the individual $\pm 1\sigma$ eigenvalues show a sizeable deviation from the central value. This is notably the case for eigenvector 1 (PDF eigenvalues 1 and 2 in Fig. 3), in which the

dominant contribution is due to the u-valence quark, and eigenvector 3 (PDF eigenvalues 5 and 6), in which the most important contribution is due to the d-valence quark. These eigenvectors impact W boson measurements at the Tevatron, in particular, the W mass measurement. Another large variation is visible for PDF eigenvector 5 (eigenvalues 9 and 10) in which the dominant contribution is due to sea quarks and gluons. This eigenvector is important for the W rapidity distribution at the LHC.

Recently, a calculation of R_{th} at NNLO became available, which takes into account the spin correlation between electron and neutrino and the experimental selection of this analysis. The authors find $R_{\text{th}} = 0.9266 \pm 0.0019$, in good agreement with our measurement [26].

In summary, we have measured the W inclusive production cross section with electrons identified at large pseudorapidities $(1.2 < |\eta| < 2.8)$ to be $\sigma \times \mathcal{B} = 2796 \pm 13(\text{stat})^{+95}_{-90}(\text{syst}) \pm 162(\text{lum})$ pb. We have measured a partial cross section using forward electrons $\sigma \times \mathcal{B} \times A = 718 \pm 3(\text{stat}) \pm 21(\text{syst})$ pb and the ratio of central-electron to forward-electron partial cross sections $R_{\text{exp}} = 0.925 \pm 0.006(\text{stat}) \pm 0.032(\text{syst})$.

a

---

[a]Visiting scientist from University of Athens, 15784 Athens, Greece.
[b]Visiting scientist from University of Bristol, Bristol BS8 1TL, United Kingdom.
[c]Visiting scientist from University Libre de Bruxelles, B-1050 Brussels, Belgium.
[d]Visiting scientist from Cornell University, Ithaca, NY 14853, USA.
[e]Visiting scientist from University of Cyprus, Nicosia CY-1678, Cyprus.
[f]Visiting scientist from University College Dublin, Dublin 4, Ireland.
[g]Visiting scientist from University of Edinburgh, Edinburgh EH9 3JZ, United Kingdom.
[h]Visiting scientist from University of Heidelberg, D-69120 Heidelberg, Germany.
[i]Visiting scientist from Universidad Iberoamericana, Mexico D.F., Mexico.
[j]Visiting scientist from University of Manchester, Manchester M13 9PL, United Kingdom.
[k]Visiting scientist from Nagasaki Institute of Applied Science, Nagasaki, Japan.
[l]Visiting scientist from University de Oviedo, E-33007 Oviedo, Spain.
[m]Visiting scientist from University of London, Queen Mary College, London, E1 4NS, United Kingdom.
[n]Visiting scientist from University of California Santa Cruz, Santa Cruz, CA 95064, USA.
[o]Visiting scientist from Texas Tech University, Lubbock, TX 79409, USA.
[p]Visiting scientist from University of California, Irvine, Irvine, CA 92697, USA.
[q]Visiting scientist from IFIC (CSIC-Universitat de Valencia), 46071 Valencia, Spain.

[1] G. Altarelli, R. K. Ellis, and G. Martinelli, Nucl. Phys. **B157**, 461 (1979); J. Kubar-Andre and F. E. Paige, Phys. Rev. D **19**, 221 (1979); K. Harada, T. Kaneko, and N. Sakai, Nucl. Phys. **B155**, 169 (1979); **B165**, 545(E) (1980); J. Abad and B. Humpert, Phys. Lett. **80B**, 286 (1979); B. Humpert and W. L. van Neerven, Phys. Lett. **85B**, 293 (1979).

[2] R. Hamberg, W. L. van Neerven, and T. Matsuura, Nucl. Phys. **B359**, 343 (1991); **B644**, 403(E) (2002); R. V. Harlander and W. B. Kilgore, Phys. Rev. Lett. **88**, 201801 (2002).

[3] S. Frixione and M. L. Mangano, J. High Energy Phys. 05 (2004) 056.

[4] CDF uses two coordinate systems: Cartesian and cylindrical. In the Cartesian system z is the beam axis, oriented in the proton direction, and x and y define the plane perpendicular to the z axis. In the cylindrical system the z axis is the same, θ is the polar angle, ϕ is the azimuthal angle, and pseudorapidity $\eta = -\ln[\tan(\theta/2)]$. Transverse energy and momentum are defined as $E_T = E\sin\theta$ and $p_T = p\sin\theta$, where E is energy measured by the calorimeter and p is momentum measured by the spectrometer. The missing E_T ($\vec{\not{E}}_T$) is defined by $\vec{\not{E}}_T = -\sum_i E_T^i \hat{n}_i$, where $\hat{n}_i$ is a unit vector perpendicular to the beam axis and pointing at the ith calorimeter tower. We also define $\not{E}_T = |\vec{\not{E}}_T|$. The transverse mass is $M_T c^2 = \sqrt{2E_T \not{E}_T(1-\cos\Delta\phi)}$, where $\Delta\phi$ is the azimuthal angle between the electron and the $\not{E}_T$.

[5] M. Dittmar, F. Pauss, and D. Zurcher, Phys. Rev. D **56**, 7284 (1997).

[6] D. Acosta et al. (CDF Collaboration), Phys. Rev. D **71**, 051104 (2005).

[7] D. Acosta et al. (CDF Collaboration), Phys. Rev. Lett. **94**, 091803 (2005). In this analysis the central-electron candidate is required to be measured by the central EM calorimeter and no requirement on its η is set.

[8] D0 Collaboration, D0 Note No. 4403-CONF, 2004.

[9] S. Abachi et al. (D0 Collaboration), Phys. Rev. D **61**, 072001 (2000).

[10] D. Acosta et al. (CDF Collaboration), Phys. Rev. D **71**, 032001 (2005).

[11] A. Sill et al., Nucl. Instrum. Methods Phys. Res., Sect. A **447**, 1 (2000); A. Affolder et al., Nucl. Instrum. Methods Phys. Res., Sect. A **453**, 84 (2000).

[12] T. Affolder et al., Nucl. Instrum. Methods Phys. Res., Sect. A **526**, 249 (2004).

[13] L. Balka et al., Nucl. Instrum. Methods Phys. Res., Sect. A **267**, 272 (1988); M. Albrow et al., Nucl. Instrum. Methods Phys. Res., Sect. A **480**, 524 (2002).

[14] G. Apollinari et al., Nucl. Instrum. Methods Phys. Res., Sect. A **412**, 515 (1998).

[15] D. Acosta et al., Nucl. Instrum. Methods Phys. Res., Sect. A **461**, 540 (2001).

[16] S. Klimenko, J. Konigsberg, and T. M. Liss, Fermilab 6 Report No. FERMILAB-FN-0741, 2003.

[17] B. L. Winer, Int. J. Mod. Phys. A **16**, 1169 (2001), supplement 01C.

[18] K. Anikeev et al., Comput. Phys. Commun. **140**, 110 (2001).

[19] A. Abulencia et al. (CDF Collaboration), arXiv:hep-ex/0508029 [Phys. Rev. D. (to be published)].

[20] C. Hays et al., Nucl. Instrum. Methods Phys. Res., Sect. A **538**, 249 (2005).

[21] T. Sjöstrand et al., Comput. Phys. Commun. **135**, 238 (2001). We use PYTHIA version 6.216.

[22] R. Brun and F. Carminati, CERN Program Library Long Writeup No. W5013, 1993 (unpublished), version 3.15.

[23] C. Anastasiou et al., Phys. Rev. D **69**, 094008 (2004).

[24] A. D. Martin et al., Eur. Phys. J. C **28**, 455 (2003).

[25] J. Pumplin et al., J. High Energy Phys. 07 (2002) 012.

[26] K. Melnikov and F. Petriello, Phys. Rev. D **74**, 114017 (2006).